Turkish Journal of Earth Sciences

http://journals.tubitak.gov.tr/earth/

Research Article

Turkish J Earth Sci
(2016) 25: 242-255

doi:10.3906/yer-1511-6

Comparison between natural radioactivity levels and geochemistry of some granitoids in western Turkey

Sibel TATAR ERKÜL[1,*], Süleyman Fatih ÖZMEN[2,3], Fuat ERKÜL[4], İsmail BOZTOSUN[3,5]
[1]Department of Geological Engineering, Faculty of Engineering, Akdeniz University, Antalya, Turkey
[2]Department of Nuclear Physics, Vocational School of Technical Sciences, Akdeniz University, Antalya, Turkey
[3]Nuclear Science Application and Research Center, Akdeniz University, Antalya, Turkey
[4]Vocational School of Technical Sciences, Akdeniz University, Antalya, Turkey
[5]Department of Physics, Akdeniz University, Antalya, Turkey

Received: 12.11.2015 • **Accepted/Published Online:** 08.03.2016 • **Final Version:** 05.04.2016

Abstract: Granitoids commonly include K-feldspar, biotite and zircon, apatite, titanite, allanite, and xenotime crystals, which are known to contain common radioactive elements. Radioactive isotopes of ^{40}K, ^{238}U, and ^{232}Th can be harmful to human health with increasing dosage and their quantification should be well defined to assess the suitability of wall-rock granitoids for indoor and outdoor purposes. In this study, it is aimed to correlate the possible relationship between concentrations of natural radionuclides and SiO_2, Na_2O, K_2O, and CaO together with elements U, Th, Zr, Y, Ba, Rb, and Sr to provide a basic approach to the compatibility of geochemical data with natural radioactivity levels of granitic to dioritic rocks in western Turkey. ^{226}Ra, ^{228}Ac, and ^{40}K radioactivity concentrations of the granitoid samples from seven locations range between 15.6 ± 1.5 and 139.7 ± 11.2, 12.0 ± 1.1 and 93.4 ± 9.0, and 297.5 ± 15.5 and 880.2 ± 47.5 Bq/kg, respectively. The lowest ^{226}Ra, ^{228}Ac, and ^{40}K values occur in the Karaburun granitoids while the Buldan granitoids have the highest values. Our data confirm that the silica-rich acidic granitoids have higher natural radioactivity levels than silica-poor basic granitoids and high natural radioactivity levels have been closely associated with high SiO_2, Na_2O, K_2O, Rb, and Ba contents, which may be explained by postmagmatic events of metasomatism and alteration. CaO, Sr, Y, and Zr do not show any correlation with natural radioactivity levels. Natural radioactivity parameters of the studied granitoids are within the safe dosage limits specified in international standards and are safe for use as construction materials. However, metasomatized or strongly altered granitoids may have elevated natural radioactivity levels and hence careful attention is needed for such granitoids.

Key words: Natural radioactivity, major and accessory minerals, geochemistry, gamma-ray spectrometry, metamorphism, metasomatism, alteration

1. Introduction

Elements U, Th, and K are much more abundant in granitoid rocks that form the significant part of the continental crust (Taylor and McLennan, 1985) and the natural terrestrial radioactivity is linked to the naturally occurring radium (^{226}Ra), actinium (^{232}Th), and potassium (^{40}K) isotopes. Granitoids contain natural ^{226}Ra, ^{232}Th, and ^{40}K unstable isotopes and radioactive elements can be incorporated into the continental crust by magmatic processes that involve partial melting and fractional crystallization. Late-phase alteration occurring after granitoid emplacement also causes excessive enrichment and relative abundance of radioactive elements (Alharbi et al., 2011; El Feky et al., 2011). Granitoids, which include abundant zircon, titanite, monazite, xenotime, apatite, and allanite minerals, are more enriched in U, Th, and K compared to upper crust and mantle reservoirs (Mason and Moore, 1982; Taylor and McLennan, 1985; Faure, 1986; Turcotte and Schubert, 2002; Örgün et al., 2007; Middlemost, 2013). Potassium is the major constituent of K-feldspar and mica minerals and has only ^{40}K, a radioactive and known long-lived isotope. Enrichment of potassium appears to have been mainly controlled by syn- to postmagmatic processes during crystallization and alteration of potassium feldspar and biotite minerals (De Capitani et al., 2007). High natural radioactivity levels in granitoids have been attributed to the U, Th, and K enrichment within accessory minerals of zircon, apatite, etc. and the major mineral phase formed by K-feldspar and biotite (Blundy and Wood, 2003). Radiation measurements can be evaluated together with whole-rock geochemical data to investigate the possible correlation between major/trace elements and natural

* Correspondence: sibel582@gmail.com

radioactivity values. Radioactivity of Ra, Th, and K isotopes of industrial granite should be evaluated with care as these elements elevate the natural radioactivity doses (Rogers and Ragland, 1961; Doventon and Prensky, 1992). Variably composed granitoid rocks studied here may provide a database to evaluate the future potential for industrial use (Rizzo et al., 2001; Tzortzis et al., 2003; Ahmed, 2005; Pavlidou et al., 2006; Kovler, 2012). As widespread occurrences of granitoids in western Turkey have high potential to be used as building material due to increasing demand for the natural stones, it is also necessary to define the negative effects of radiation in industrial granitoids for human health (Örgün et al., 2005, 2007; Osmanlıoğlu et al., 2006; Canbaz et al., 2010; Karadeniz et al., 2011; Çetin et al., 2012; Sayın, 2013; Karadeniz and Akal, 2014; Öztürk et al., 2015). This study deals with the determination of natural radioactivity levels and geochemical analysis of distinct granitoid bodies in order to reveal the possible relationship between particular elements and natural background radioactivity levels and to assess the suitability of some granitoid rocks in western Turkey in terms of natural radiation.

2. Geological outline and petrography

Granitoids exposed in western Turkey have variable compositions from granite to tonalite and have the potential to be used as building materials. They occurred in different tectonic settings and time intervals since Pre-Cambrian to Miocene times (Delaloye and Bingöl, 2000). In this study, granitoids in the Buldan, Karaburun, Alaçamdağ, Eğrigöz, Koyunoba, Salihli, and Turgutlu areas, which have been or are being studied geologically in some detail, have been sampled for geochemical analyses and natural activity measurements (Figure 1).

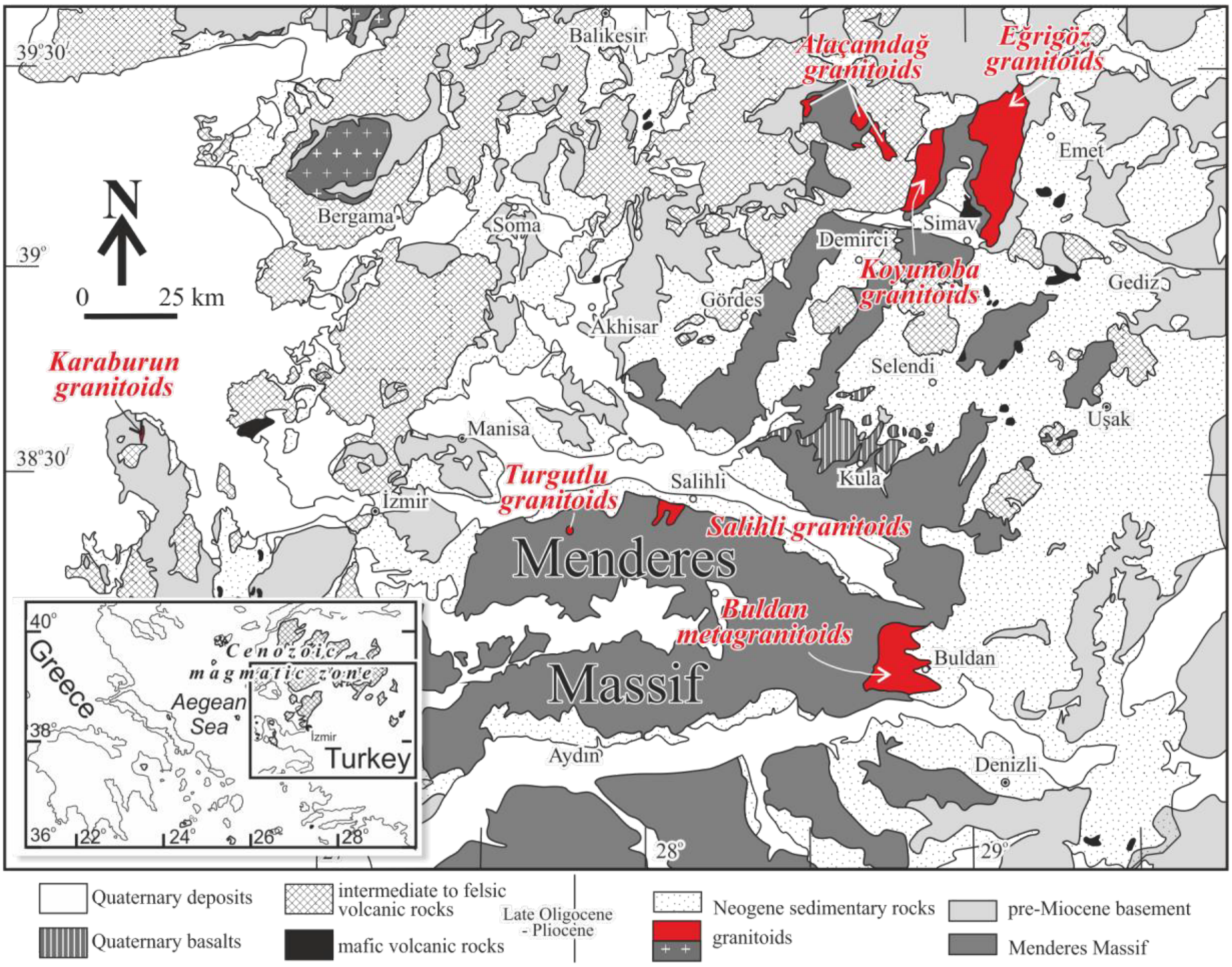

Figure 1. Generalized geological map of western Turkey including major basement rocks and volcanic/plutonic suites together with Cenozoic sedimentary basins [modified from Geological Map of Turkey-İzmir, Denizli (1:500.000) (MTA, 1964)]. Red-colored outcrops indicate the studied granitoids.

Granitoid rocks in the Buldan area were entirely metamorphosed while other granitoid occurrences are unmetamorphosed with lacking or slight deformation. The Buldan area is underlain by metagranitoids of the Menderes Massif formed by augen gneisses, porphyritic granites, and tourmaline-bearing metagranites (Figure 1) (Erkül and Erkül, 2012). Augen gneisses are characterized by local occurrences of large, euhedral, and slightly deformed K-feldspar megacrysts. Porphyritic granites are mineralogically similar to those of the augen gneisses but display less amounts of deformation and foliation planes. Tourmaline-bearing metagranites are defined by abundant tourmaline nodules surrounded by quartz and feldspar crystals. All these granitoids include a significant amount of zircon crystals as an accessory phase. Granitoids in the Karaburun area occur as small stocks and their chemical composition ranges from tonalite and diorite to minor granodiorite (Erkül et al., 2008). Apatite, titanite, and zircon are common accessory minerals in these plutons. Granitoids in the Alaçamdağ area are mainly granodiorite to minor granite in composition (Erkül, 2012; Erkül and Erkül, 2012). They are commonly equigranular and locally porphyritic, and they include accessory phases of zircon and allanite. The geological outline together with radiological mapping of the Eğrigöz pluton has already been described by Öztürk et al. (2015). Lithological and mineralogical characteristics of the Koyunoba and Eğrigöz granitoids are closely similar to those exposed in the Alaçamdağ area. They have typical granite and granodiorite mineral assemblages and include abundant zircon, apatite, and allanite as accessory phase, but the Koyunoba granite differs from the Alaçamdağ and Eğrigöz granites by the absence of hornblende crystals. Granitoids in the Salihli area consist of granodiorites with less tonalites. Although they are commonly equigranular, foliation planes locally occur on the structurally upper parts. Accessory minerals in the Salihli granitoids are made up of titanite, apatite, zircon, and tourmaline (Erkül et al., 2013). Mineralogical composition of the Turgutlu granitoids closely resembles that of the Salihli granitoids, but minor hornblende crystals and common accessory minerals of allanite and zircon crystals are observed.

These granitoid bodies can be classified by their distinctive geological, mineralogical, and geochemical characteristics, which allow us to compare the natural radioactivity levels of intrusive plutons to other parameters. These parameters include age (geochronological constraints), mineralogical and geochemical composition, an abundance of rock-forming minerals and radioactive element-bearing accessory minerals, geographic location in western Turkey, and the degree of alteration and metamorphism (Table 1).

3. Materials and methods

A total of 25 fresh granitoid samples of approximately 1–2 kg were collected from seven locations in western Turkey (Figure 1). Petrographic studies were carried out on thin sections to describe the mineralogical composition and alteration mineralogy of the granitoid samples using a Nikon Labophot under a light polarized microscope. Samples collected for geochemical analysis and radioactivity measurements were crushed and homogenized with the grinding machine in the Akdeniz University Department of Geological Engineering, Mineralogy-Petrography Laboratory, Turkey. Granitoid samples were analyzed for whole-rock major and trace element compositions at ACME Laboratories in Vancouver, Canada (Erkül et al., 2008, 2013; Erkül and Erkül, 2012) (Table 2).

Approximately 250 g of rock powders from each sample were filled in hermetically sealed cylindrical containers of 5 cm in diameter. Containers of 150 mL with ground samples were labeled, weighed, and stored for about 4 weeks in order to reach secular equilibrium between ^{226}Ra and ^{222}Rn prior to counting. Radiation measurements were completed in the gamma-ray spectroscopy laboratory in the Physics Department at Akdeniz University. An HPGe gamma-ray detector on a gamma-ray spectrometer [AMATEK-ORTEC (GEM40P4-83)] was used for radioactivity measurements. The resolution of the detector is 768-eV full width at half maximum (FWHM) at 122 keV for ^{57}Co and 1.85-keV FWHM at 1332 keV for ^{60}Co with a relative efficiency of 40%. Calibration standards and data acquisition procedures were the same as applied by Özmen et al. (2013). The energy calibration of the spectrometer was performed using a mixed calibration source supplied by the Çekmece Nuclear Research and Training Center (IAEA 1364-43-2) emitting gamma rays in the energy range between 47 and 1836 keV for efficiency calibration with the same geometry as the samples. The source contained 11 radionuclides in 1.3-gcc 21 epoxy matrix (^{210}Pb, ^{241}Am, ^{109}Cd, ^{57}Co, ^{139}Ce, ^{203}Hg, Sn, ^{85}Sr, ^{88}Y, ^{60}Co, and ^{137}Cs). All samples were placed to the front face of the detector and counted for 50,000 s. Background intensities were obtained with an empty container for 50,000 s under the same conditions before and after measurement of the samples. The average of the background counts was then subtracted from the sample spectrums. Then the efficiency vs. energy graphs were plotted and fitted to the equation of Gilmore (2008):

$$Eff(E) = a + b \times log(E) + c \times log(E)^2 + d \times log(E)^3 \quad (1)$$

where a, b, c, and d are the best-fit parameters determined by the fitting algorithm. Finally, the efficiency values used in the activity concentration calculation of the full energy peaks were calculated by using Eq. (1).

Table 1. General characteristics of the studied granitoids in western Turkey.

Sample	Age	Rock type	Mineralogical composition (weight %, CIPW norm)			Distinct mineralogical and/or geochemical characteristics	Metamorphism/alteration
			Quartz	K-bearing minerals	Accessory minerals		
Buldan area							
BGR-1	Precambrian	Augen gneiss	39	27	0.33	Enriched in silica- and K-bearing minerals compared to other granitoids; highest SiO_2 and K_2O contents	Multistage regional metamorphism and metasomatism
BGR-2		Augen gneiss	39	20	0.24		
BGR-3		Augen gneiss	32	28	0.31		
BRL-1		Leucogranite	33	25	0.15		
BRL-2		Leucogranite	31	25	0.31		
BRP-1		Porphyritic granite	32	20	0.47		
Average			34	24	0.31		
Karaburun area							
KBR-1	Triassic	Granodiorite	22	15	0.26	Depleted in Zr and U; low abundance of K-bearing minerals	Slight propylitic alteration
KBR-2	Triassic	Granodiorite	18	9	0.29		
Average			20	12	0.28		
Alaçamdağ area							
AWR-1	Early Miocene	Granite	28	22	0.31	Slightly enriched in Th relative to the other granitoids	Almost completely unaltered
AWR-2			28	21	0.31		
AWR-3			26	20	0.35		
AWR-4			27	24	0.35		
AWR-5			24	18	0.28		
Average			27	21	0.32		
Eğrigöz area							
EMR-1	Precambrian	Metagranite	24	21	0.66	Abundant accessory minerals	Metamorphosed
ER-1	Early Miocene	Granite	24	23	0.46		Almost completely unaltered
ER-2			26	26	0.41		
ER-3			29	25	0.35		
Average			26	24	0.47		
Koyunoba area							
KR-1	Early Miocene	Granite	29	27	0.22	Relatively enriched in K-bearing minerals	Very slightly altered
KR-2			29	27	0.31		
KR-3			30	27	0.26		
Average			29	27	0.26		
Salihli area							
SR-1	Middle Miocene	Granodiorite	27	18	0.34	Relatively low abundance of K-bearing minerals	Unaltered
SR-2			29	14	0.36		
SR-3			25	17	0.36		
SR-4			25	17	0.34		
Average			27	17	0.35		
Turgutlu area							
TR-1	Middle Miocene	Granodiorite	28	23	0.35	Lowest Y content	Unaltered

Table 2. Representative whole-rock major and trace element geochemical analyses of the granitoid samples in western Turkey.

Sample no.	Lithology	SiO_2	Al_2O_3	Fe_2O_3	MgO	CaO	Na_2O	K_2O	TiO_2	P_2O_5	MnO	LOI*	Total	Ba	Rb	Sr	Th	U	Zr	Y
Buldan area		Major oxides (weight %)												Trace elements (ppm)						
BGR-1	Augen gneiss	76.04	12.63	1.52	0.34	0.41	3.12	4.64	0.19	0.13	0.02	0.98	100.00	273.7	228.3	50.6	24.1	4.6	127.2	41.9
BGR-2	Augen gneiss	75.49	13.17	1.62	0.42	0.34	3.81	3.39	0.20	0.09	0.01	1.45	99.98	185.6	183.9	50.7	28.6	6.3	137.8	47.4
BGR-3	Augen gneiss	72.81	14.03	1.92	0.42	0.60	3.60	4.77	0.27	0.12	0.04	1.30	99.89	575.4	160.1	57.7	26.0	2.9	179.1	41.8
BRL-1	Leucogranite	74.62	13.35	1.83	0.14	1.02	3.88	4.28	0.16	0.05	0.02	0.60	99.94	556.8	128.4	71.5	20.1	4.5	183.8	53.6
BRL-2	Leucogranite	71.56	14.31	1.91	0.99	1.70	3.31	4.30	0.43	0.12	0.02	1.10	99.75	655.5	193.0	191.2	31.8	9.6	171.4	38.0
BRP-1	Porphyritic granite	69.93	14.02	3.18	1.77	1.84	3.18	3.52	0.57	0.19	0.03	1.70	99.95	531.9	135.1	220.7	9.7	3.0	177.9	27.3
Karaburun area																				
KBR-1	Granodiorite	60.91	14.27	6.46	4.04	5.42	2.22	2.60	0.50	0.11	0.11	3.30	99.93	370.6	97.7	205.1	7.2	1.7	108.6	18.2
KBR-2	Granodiorite	56.89	14.12	8.27	5.63	7.11	2.16	1.44	0.59	0.12	0.13	3.43	99.93	302.2	48.8	234.0	6.5	1.4	93.6	18.0
Alaçamdağ area																				
AWR-1	Granite	67.99	15.52	3.28	1.10	3.14	3.08	3.71	0.40	0.12	0.07	1.40	99.80	795.1	136.4	258.4	12.5	4.5	158.8	24.6
AWR-2	Granite	68.37	15.72	3.38	1.12	3.10	3.30	3.54	0.40	0.12	0.06	0.77	99.89	838.5	138.5	280.4	14.3	3.7	160.2	24.0
AWR-3	Granite	67.29	15.86	3.52	1.47	3.43	3.33	3.37	0.47	0.14	0.07	0.90	99.83	765.1	132.1	322.6	11.8	5.3	154.2	23.4
AWR-4	Granite	69.19	15.32	2.81	1.08	2.81	3.37	4.05	0.38	0.14	0.06	0.65	99.86	1008.5	135.9	384.5	16.6	7.3	148.9	22.5
AWR-5	Granite	65.31	15.56	4.29	1.85	4.06	3.16	3.08	0.54	0.11	0.08	1.70	99.74	666.7	124.4	330.5	15.3	4.9	142.7	25.1
Eğrigöz area																				
EMR-1	Metagranite	65.74	16.24	3.67	1.39	3.51	3.34	3.55	0.44	0.27	0.06	1.30	99.51	1845.3	117.1	838.1	19.9	9.6	160.3	26.5
ER-1	Granite	67.15	15.39	3.53	1.22	2.86	3.49	3.91	0.52	0.18	0.07	1.30	99.65	1088.7	138.8	327.1	19.9	4.8	196.8	24.7
ER-2	Granite	68.47	14.75	3.17	1.10	2.46	3.24	4.32	0.48	0.16	0.06	1.43	99.66	1117.0	159.3	285.8	19.4	5.0	194.7	25.0
ER-3	Granite	70.34	14.34	2.59	0.86	2.15	3.34	4.29	0.39	0.14	0.06	1.23	99.68	885.0	158.9	242.3	23.6	7.1	176.2	22.7
Koyunoba area																				
KR-1	Granite	72.24	14.14	1.93	0.40	1.31	3.74	4.62	0.20	0.08	0.05	0.97	99.66	943.0	171.9	174.1	21.3	3.9	177.1	22.0
KR-2	Granite	71.53	14.60	1.86	0.54	1.63	3.59	4.50	0.26	0.12	0.05	1.03	99.68	987.0	173.3	241.2	19.6	5.4	154.7	20.8
KR-3	Granite	72.09	14.44	1.92	0.40	1.22	3.71	4.65	0.22	0.10	0.06	0.90	99.70	1006.0	175.5	193.7	20.1	3.3	181.1	23.0
Salihli area																				
SR-1	Granodiorite	67.67	15.81	3.20	1.26	3.65	3.20	3.19	0.51	0.13	0.06	1.07	99.77	602.7	105.9	344.8	14.5	4.2	185.1	17.1
SR-2	Granodiorite	66.03	16.15	3.73	1.50	3.90	3.00	2.44	0.60	0.14	0.07	2.20	99.77	493.3	75.8	362.9	16.3	3.6	201.3	20.8
SR-3	Granodiorite	65.11	16.19	4.10	1.91	4.38	2.99	2.80	0.69	0.14	0.08	1.40	99.77	462.8	106.1	326.4	18.1	3.3	193.4	19.6
SR-4	Granodiorite	65.87	16.21	3.83	1.68	4.27	3.13	2.86	0.66	0.13	0.07	1.04	99.78	483.2	105.7	349.8	13.0	3.4	192.1	21.8
Turgutlu area																				
TR-1	Granodiorite	69.75	15.75	2.65	0.78	2.50	3.51	3.83	0.33	0.14	0.07	0.65	100.00	590.0	142.5	275.9	12.3	3.5	130.5	15.2

*Loss on ignition.

^{226}Ra and ^{232}Ac activity concentrations were determined from their daughter products indirectly while ^{40}K was determined directly by its characteristic gamma ray peaks. To determine the activity concentration of ^{226}Ra nuclide, daughter nuclides ^{214}Pb and ^{214}Bi were used, while ^{228}Ac concentration was chosen for the parent ^{232}Th. The gamma transitions of 242, 295.2, and 351.9 keV ^{214}Pb and 609.3, 1120.3, and 1764.5 keV ^{214}Bi were used to determine the concentrations of ^{226}Ra. The gamma transition of 911.2 keV ^{228}Ac was used to determine the concentration of ^{232}Th. The gamma transition of 1461.0 keV was used to determine the concentration of ^{40}K. The activity concentration of the radionuclides in the analyzed samples was calculated by the following well-known equation:

$$\Lambda = N/(\varepsilon \times P \times t \times m) \qquad (2)$$

where N is the net counts under the full energy peaks, ε is the detector efficiency of the specific energy, P is the probability of gamma decay, t is the counting live-time (s), and m is the mass of sample (kg). Minimum detectable activities (Gilmore, 2008) of the measurement system for ^{214}Pb, ^{214}Bi, ^{232}Th, and ^{40}K radionuclides are given in Table 3 for 1 kg sample size and 50,000 s live counting time.

4. Results and discussion

4.1. Classification and whole-rock geochemical characteristics of granitoids

Whole-rock major and trace element chemical contents of granitoids in western Turkey are given in Table 1. When the normative mineralogical composition of these granitoid samples is plotted on the QAP classification (Streckeisen, 1976), they fall into the granite, granodiorite, and tonalite fields (Figure 2). The studied granitoids in western Turkey commonly have high-K, calc-alkaline, transitional metaluminous to peraluminous and I-type character, except for the Buldan metagranitoids with S-type and peraluminous affinity (Erkül et al., 2008, 2013; Erkül, 2012). The Buldan metagranitoids have SiO_2 contents ranging from 69.93 to 76.04 wt. % with an average of 73.41 wt. %. TiO_2 contents are within the range of 0.16 and 0.57 wt. %, averaging 0.30 wt. %. The total weight percentage of iron oxides is between 1.52 and 3.18 with an average of 1.20 wt. %, which is elevated by ferromagnesian and opaque minerals within the porphyritic metagranites. Na_2O and K_2O of these metagranitoids have an average of 3.48 and 4.15 wt. %, respectively.

Karaburun granitoid samples have the lowest SiO_2 contents among the studied granitoids, ranging from 56.89 to 60.91 wt. %, and their TiO_2 contents are higher than most of the granitoids except for the Salihli granodiorite, averaging between 0.50 and 0.59 wt. %. They are characterized by the highest total iron oxide (6.46–8.27 wt. %, average 7.40 wt. %) and lowest Na_2O (2.16–2.22 wt. %, average 2.19 wt. %) and K_2O contents (1.44–2.60 wt. %, average 2.02 wt. %). The Alaçamdağ and Eğrigöz granitoids are relatively low in SiO_2 (63.31–69.19 wt. %, average 67.63 wt. % and 65.74–70.34 wt. %, average 67.93 wt. %) and high in total iron oxide (2.81–4.29 wt. % with an average of 3.5 wt. % in the Alaçamdağ and 2.59–3.67 wt. % with an average of 3.24 wt. % in the Eğrigöz granitoids) contents compared to the Buldan metagranitoids. TiO_2, Na_2O, and K_2O contents in the Alaçamdağ and Eğrigöz granitoids are similar to those of the Buldan metagranitoids. All the rock samples analyzed from the Koyunoba granitoids have higher SiO_2 (71.53–72.24 wt. %, average 71.95 wt. %), lower TiO_2 (0.20–0.26 wt. %, average 0.23 wt. %), and lower total iron oxide (1.86–1.93 wt. %, average 1.90 wt. %) with respect to the Alaçamdağ and Eğrigöz granitoids. Na_2O and K_2O of the Koyunoba granite range from 3.5 to 3.71 wt. % with an average of 3.68 wt. % and 4.50 to 4.65 wt. % with an average of 4.59 wt. %, respectively. These results are also comparable to those of the Alaçamdağ and Eğrigöz granitoids. Whole-rock geochemical data from the Salihli granitoids also display close similarities to the Alaçamdağ and Eğrigöz granitoids. However, it is noteworthy that the TiO_2 (>0.51 wt. %) contents of the Salihli granitoids are the highest among the studied granitoids. Turgutlu granitoids differ from the Salihli granitoids with their low Fe_2O_3, MgO, CaO, and TiO_2, and slightly higher Na_2O and K_2O contents. Trace element contents of the studied granitoids are characterized by highest Rb, Th, and Y in the Buldan metagranitoids and highest Ba, Sr, U, and Zr in the Eğrigöz granites. The Karaburun granodiorites differ from other granitoids with their low Rb, Ba, Th, U, and Zr contents.

4.2. Gamma radioactivity concentrations of granitoids

Zr, Th, U, and Y are concentrated in the accessory minerals, i.e. zircon, apatite, monazite, and titanite (Pagel, 1982). Th versus U diagrams indicate that U content of granitoid samples increases with increasing Th content (Figure 3a). In the variation diagram of Th versus Th/U, Th remains constant with increasing Th/U ratio (Figure 3b). The U versus Th/U diagram displays increasing Th/U ratio with decreasing U (Figure 3c). These correlations indicate that the granitoid rocks have relatively minor variation in Th content while the U content of these rocks appears to be

Table 3. Minimum detectable activities of ^{214}Pb, ^{214}Bi, ^{228}Ac, and ^{40}K radionuclides for 1 kg sample size and 50,000 s live counting time.

Radionuclide	Energy (keV)	MDA (Bq/kg)
^{214}Pb	352	0.53
^{214}Bi	609	0.85
^{228}Ac	911	1.72
^{40}K	1461	18.48

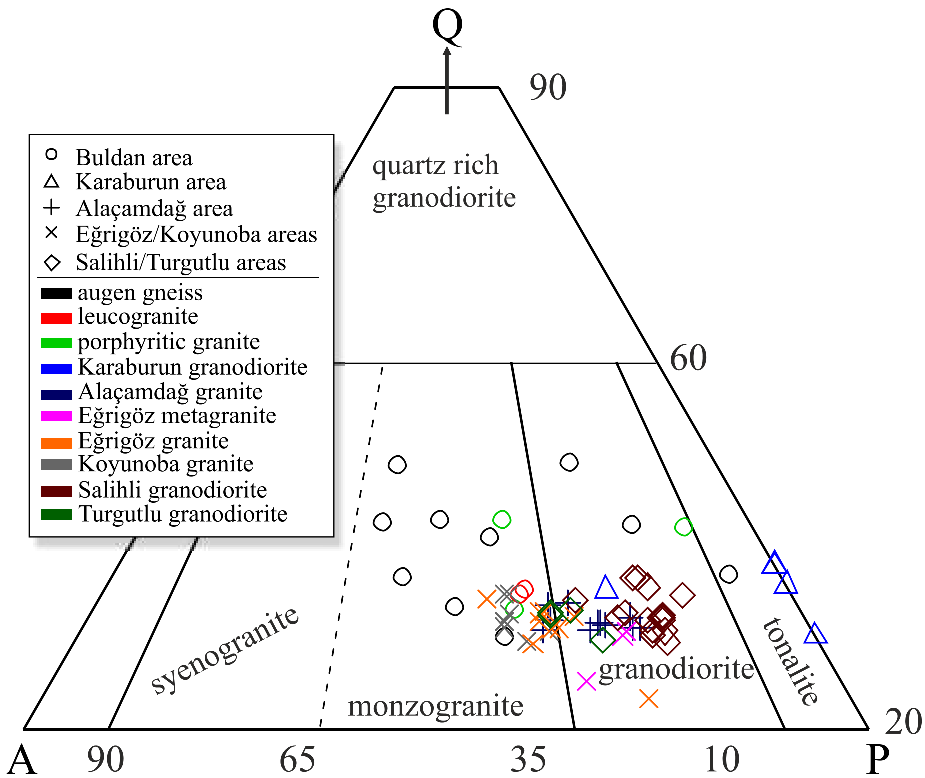

Figure 2. Quartz-alkali feldspar-plagioclase (QAP) classification diagram (Streckeisen, 1976) of granitoids in western Turkey.

highly variable. This can be explained by the disintegration of U into Th during late-stage processes (Papadopoulos et al., 2013). The Zr versus SiO_2 variation diagram reveals that the Zr content increases with increasing SiO_2, from intermediate to acidic granitoids (Figures 3d–3f), which is common in worldwide granitoids (cf. Rankama and Sahama, 1950). Zr depletion with respect to SiO_2 within two samples of the Buldan granitoids is also noteworthy. This can be caused by relative enrichment of silica with respect to Zr (Figure 3d). In Zr/U versus U and Zr/Th versus Th binary diagrams, Zr is depleted relative to U and Th contents (Figures 3e and 3f). Because the U ion is about the same size as the Zr ion, U will substitute for Zr and crystallize in zircon (Collins, 1999).

Na_2O, K_2O, CaO, Rb, Ba, and Sr are major constituents or commonly occur within the alkali feldspars. Rb occurs as a minor trace element constituent in alkali feldspars and biotites. Rb has a typically increasing trend with K_2O while Na_2O decreases (Deer et al., 2001). Rb is commonly included within the crystal structure of potassium feldspar and enriched in late-phase acidic granitoids. On the other hand, metasomatic and metamorphic processes may typically lead to the increase in SiO_2 and K_2O together with Rb and cause relative depletion of radioactive elements within the accessory minerals. Ba occurs as a minor to major constituent in alkali feldspars. The element Sr that acts in a similar behavior with CaO is variable in concentrations. Therefore, some major and trace elements that may be linked to the concentration of natural radionuclides have been used in the variation diagrams (Attendorn and Bowen, 1994).

Measurements for ^{226}Ra, ^{228}Ac, and ^{40}K activity concentration of granitoid samples are presented in Table 4 and Figures 4a–4k. The activity concentrations of ^{226}Ra, ^{228}Ac, and ^{40}K ranges respectively from 15.6 ± 1.5 to 139.7 ± 11.2 Bq/kg with a mean of 64.1 Bq/kg, 12.0 ± 1.1 to 93.4 ± 9.0 Bq/kg with a mean of 52.8 Bq/kg, and 297.5 ± 15.5 to 880.2 ± 47.5 Bq/kg with a mean of 748.9 Bq/kg. The highest ^{226}Ra, ^{228}Ac, and ^{40}K activity concentrations investigated were 139.7 ± 11.2 Bq/kg for sample BGR-1, 93.4 ± 9 Bq/kg for sample ER-3, and 880.2 ± 47.5 Bq/kg for sample BGR-3, respectively. In the Zr versus ^{226}Ra diagram, Zr displays a decreasing trend while ^{226}Ra is relatively high in the granitoid samples, except for the Karaburun samples (Figure 4a). ^{226}Ra values of the granitoids are rather variable against Y content; the Buldan, Karaburun, and Eğrigöz/Koyunoba granitoids have respectively negative, positive, and horizontal trends against Y content (Figure 4b). Higher abundance and distinctive negative trends of Y plots within the Buldan granitoids may be attributed to

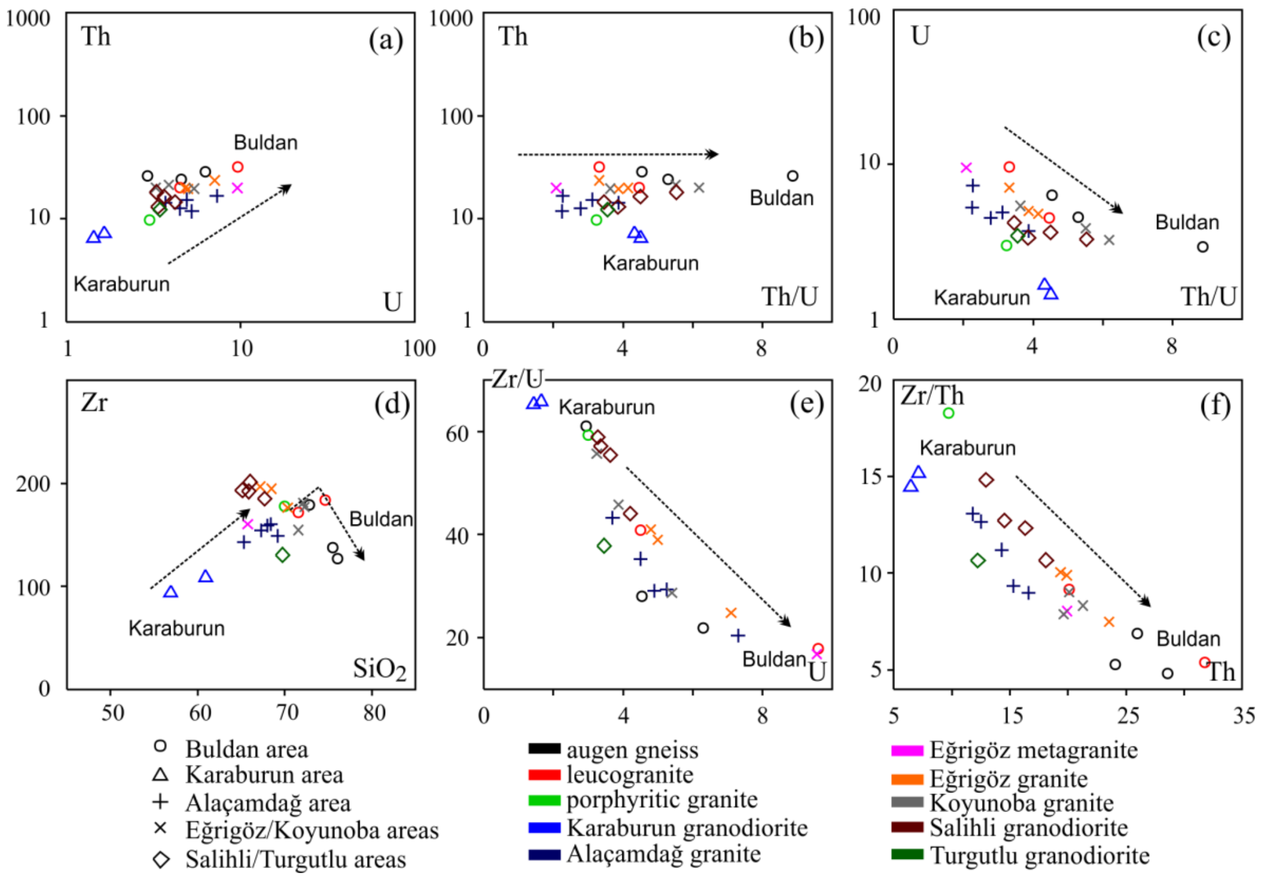

Figure 3. Variation diagrams for correlation of U, Th, Zr, and SiO_2 data from granitoids in western Turkey.

the late-stage metasomatic/metamorphic processes. Ba, Rb, and K contents within the granitoid samples increase with increasing ^{40}K (Figures 4c and 4d) while CaO and Sr display a strong depletion (Figures 4g and 4h). Na_2O plots against ^{40}K display irregular distribution (Figure 4e). High potassium contents with increasing ^{40}K values are presumed to be associated with crystallization of larger amounts of potassium feldspar. ^{226}Ra, ^{228}Ac, and ^{40}K activity concentration values increase with increasing SiO_2 contents (Figures 4i–4k).

U and Th contents of the studied granitoid plutons range from 1.4 to 9.6 and from 6.5 to 31.8 ppm, respectively. When all results are compared, U and Th contents of the analyzed samples are strongly enriched relative to the average composition of the upper continental crust (average 2.7 ppm for U and 10.5 ppm for Th) (Rudnick and Gao, 2003) (Table 2). Radionuclide concentration of ^{226}Ra ranges between 15.6 ± 1.5 and 139.7 ± 11.7 Bq/kg while ^{228}Ac ranges between 12.0 ± 1.1 and 93.4 ± 9 Bq/kg (Table 4). The significant feature of these samples is the fact that the radionuclide concentrations of ^{226}Ra (^{238}U) are higher than those of ^{228}Ac (^{232}Th) while U is much lower than Th in the granitoid samples. Th enrichment has already been pointed out in low-calcium granites, which may be linked to the fluid circulation after emplacement of granitoid plutons (Bowen, 1994). High Th contents together with activity concentrations of ^{226}Ra (^{238}U) are rather characteristic of altered or metamorphosed granites in the Buldan and Eğrigöz areas, confirming the remarkable role of the thermal metamorphism and metasomatic processes that influenced the original composition of granitoid rocks (Bieda and Lizurek, 2008).

4.3. The absorbed gamma dose rate and annual effective dose equivalent

The absorbed gamma dose rates (D in nGy/h) in air at 1 m above the ground was computed by the following equation of the United Nations Scientific Committee on the Effects of Atomic Radiation (UNSCEAR, 1993, 2000).

$$D = 0.462 \times ARa + 0.621 \times ATh + 0.0417 \times AK \quad (3)$$

where *ARa*, *ATh*, and *AK* are the concentrations of ^{226}Ra, ^{232}Th, and ^{40}K in Bq/kg respectively (Eq. (3)). During calculation, secular equilibrium was assumed to exist between radionuclides and their progeny within each series. Absorbed dose rate in the air outdoors ranged between 27.05 and 143.68 nGy/h with a mean of 88 nGy/h (Table 5). These values are within the range specified by the UNSCEAR (2000) report.

Table 4. Activity concentration of radionuclides (Bq/kg) in some granitoids of western Turkey.

Sample number	^{226}Ra	^{228}Ac	^{40}K	Ac/Ra (Th/U)
Buldan area				
BGR-1	105.7± 10.3	68.4 ± 5.6	825.9 ± 38.0	0.647
BGR-2	87.6 ± 7.5	73.1 ± 5.9	608.7 ± 32.3	0.833
BGR-3	43.4 ± 3.5	87.9 ± 8.8	880.2 ± 47.5	2.027
BRL-1	42.8 ± 4.1	58.9 ± 5.1	585.6 ± 31.6	1.374
BRL-2	84.5 ± 7.0	49.0 ± 3.9	671.3 ± 31.5	0.579
BRP-1	33.3 ± 2.9	27.6 ± 2.6	546.4 ± 24.6	0.829
Karaburun area				
KBR-1	21.8 ± 1.8	22.9 ± 2.0	524.7 ± 25.7	1.049
KBR-2	15.6 ± 1.5	12.0 ± 1.1	297.5 ± 15.5	0.764
Alaçamdağ area				
AWR-1	56.9 ± 5.1	43.2 ± 3.9	551.6 ± 24.8	0.760
AWR-2	50.9 ± 4.1	32.7 ± 2.7	535.8 ± 26.3	0.642
AWR-3	77.0 ± 6.2	45.7 ± 4.7	623.8 ± 29.3	0.593
AWR-4	99.4 ± 9.7	63.6 ± 6.0	664.0 ± 34.5	0.640
AWR-5	73.9 ± 6.1	46.0 ± 3.7	557.0 ± 27.3	0.623
Eğrigöz area				
EMR-1	139.7 ± 11.2	63.0 ± 6.3	539.9 ± 28.1	0.451
ER-1	83.3 ± 7.9	63.8 ± 5.2	713.4 ± 32.1	0.766
ER-2	61.3 ± 5.0	52.9 ± 4.3	781.6 ± 36.7	0.863
ER-3	114.3 ± 11.3	93.4 ± 9.0	788.2 ± 39.4	0.817
Koyunoba area				
KR-1	40.1 ± 3.0	82.3 ± 7.0	841.8 ± 42.1	2.054
KR-2	64.7 ± 5.2	45.5 ± 4.2	732.2 ± 38.1	0.703
KR-3	39.0 ± 3.9	86.7 ± 9.1	824.1 ± 41.2	2.220
Salihli area				
SR-1	58.1 ± 5.1	49.2 ± 4.0	591.3 ± 31.9	0.846
SR-2	55.7 ± 4.2	33.5 ± 3.5	372.8 ± 20.1	0.600
SR-3	47.6 ± 4.5	46.8 ± 3.6	535.7 ± 25.7	0.983
SR-4	49.9 ± 4.9	50.6 ± 4.6	542.6 ± 28.8	1.012
Turgutlu area				
TR-1	55.4 ± 4.9	20.7 ± 1.6	664.4 ± 29.9	0.374

Conversion factors of 0.7 Sv/Gy for adults, 0.8 Sv/Gy for children, and 0.9 Sv/Gy for infants and 0.2 as the outdoor occupancy factor were used in order to estimate the annual effective dose equivalent from the absorbed dose in the air (UNSCEAR, 2000). The annual effective dose equivalent from outdoors in units of µSv/year (UNSCEAR, 1988) is given by the following equation:

$$\text{AED } (\mu\text{Sv/year}) = D(\text{nGy/h}) \times 8760 \text{ (h/year)} \times 0.2 \times 0.7(\text{Sv/Gy}) \times 10^{-3} \quad (4)$$

The annual effective dose equivalent originating from external exposure to terrestrial radionuclides in the studied granitoids ranges from 33.17 to 176.21 µSv/year with a mean value of 108.81 µSv/year for adults, 37.91 to 201.38 µSv/year with a mean value of 124.36 µSv/year for children, and 42.65 to 226.55 µSv/year with a mean value of 139.90 µSv/year for infants.

4.4. The radium equivalent activity (Ra_{eq}), external hazard index (Hex), and gamma index (I_γ)

The gamma-ray radiation hazards arising from terrestrial radionuclides were evaluated by the indices as radium equivalent activity, external hazard index, and gamma

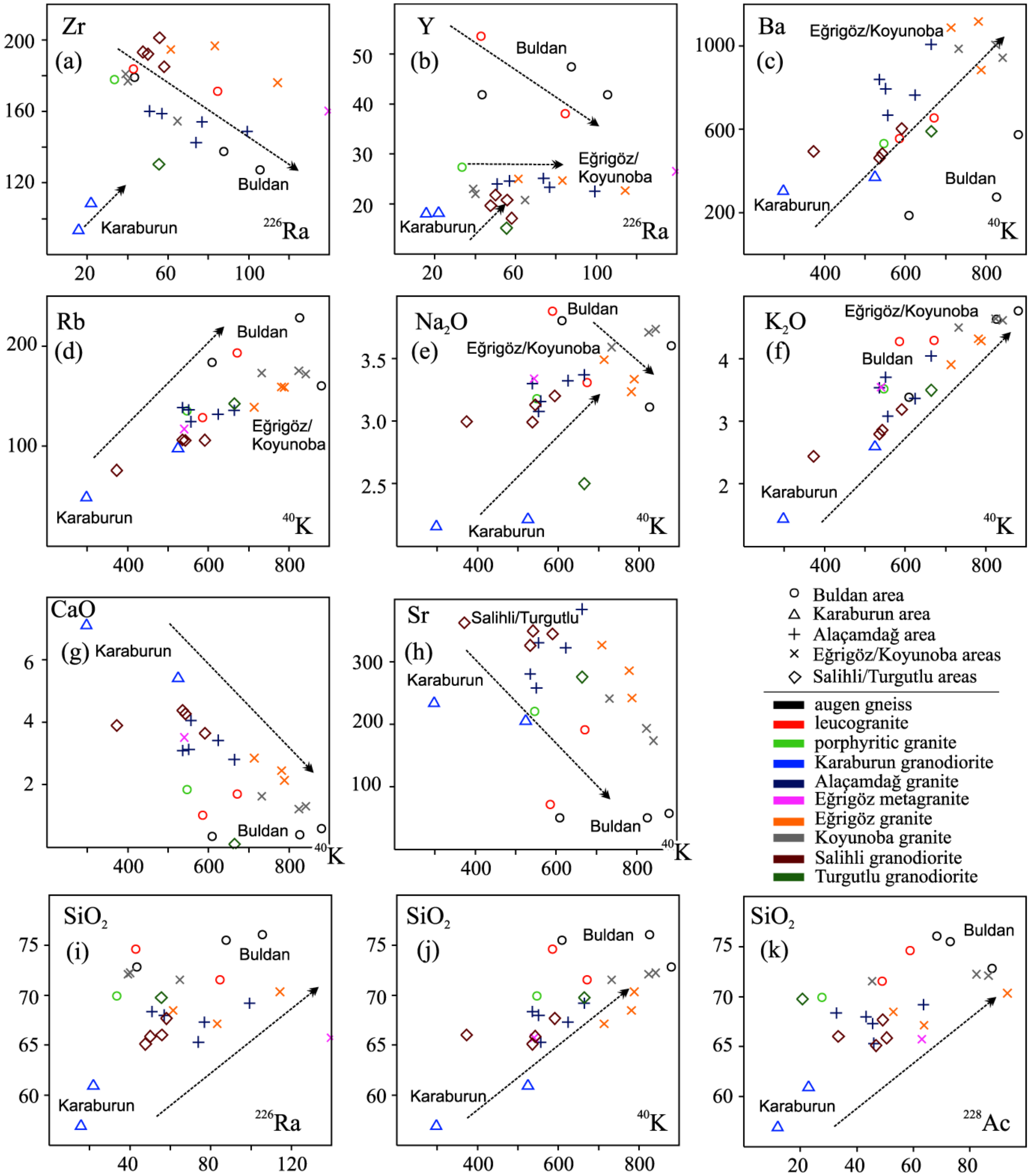

Figure 4. Variation diagrams for correlation of some trace and major elements versus ^{40}K, ^{226}Ra, and ^{228}Ac activity concentration (Bq/kg) values.

index under the assumption that 370 Bq/kg ^{226}Ra, 259 Bq/kg ^{228}Ac, and 4810 Bq/kg ^{40}K produce the same gamma-ray dose rate (Krieger, 1981; UNSCEAR, 1982; Beretka and Mathew, 1985). Ra_{eq} was calculated with the following equation:

$$Ra_{eq} = (AK \times 0.077) + (AU) + (ATh \times 1.43) \quad (5)$$

where AK, AU, and ATh are the activity concentrations of ^{40}K, ^{226}Ra, and ^{228}Ac in Bq/kg, respectively. Ra_{eq} values estimated for the collected samples are presented in Table 5. The values of Ra_{eq} varied from 55.63 to 308.55 Bq/

Table 5. Gamma dose rate (GDR), radium equivalent activity (REA), external (EHI) and internal (Iϒ) hazard index, and annual effective dose (AED) of some granitoid rocks in western Turkey.

Sample number	GDR (nGy/h)	REA (Bq/kg)	EHI	Iϒ	AED, adults (µSv/year)	AED, infants	AED, children
Buldan area							
BGR-1	125.76	267.12	0.72	0.79	154.23	198.29	176.26
BGR-2	111.24	238.98	0.65	0.71	136.42	175.40	155.91
BGR-3	111.30	236.78	0.64	0.80	136.49	175.49	155.99
BRL-1	80.77	172.12	0.46	0.56	99.06	127.36	113.21
BRL-2	97.45	206.22	0.56	0.61	119.51	153.65	136.58
BRP-1	55.33	114.90	0.31	0.38	67.86	87.25	77.56
Karaburun area							
KBR-1	46.20	95.02	0.26	0.33	56.66	72.85	64.76
KBR-2	27.05	55.63	0.15	0.18	33.17	42.65	37.91
Alaçamdağ area							
AWR-1	76.13	161.18	0.44	0.49	93.36	120.04	106.70
AWR-2	66.15	138.88	0.38	0.43	81.12	104.30	92.71
AWR-3	89.91	190.26	0.51	0.56	110.27	141.78	126.02
AWR-4	113.10	241.45	0.65	0.71	138.70	178.33	158.52
AWR-5	85.96	182.63	0.49	0.54	105.42	135.55	120.49
Eğrigöz area							
EMR-1	126.22	271.46	0.73	0.73	154.80	199.02	176.91
ER-1	107.81	229.37	0.62	0.70	132.22	170.00	151.11
ER-2	93.77	197.14	0.53	0.63	115.00	147.85	131.43
ER-3	143.68	308.55	0.83	0.92	176.21	226.55	201.38
Koyunoba area							
KR-1	104.75	222.64	0.60	0.76	128.47	165.17	146.82
KR-2	88.65	186.07	0.50	0.58	108.72	139.78	124.25
KR-3	106.21	226.41	0.61	0.77	130.26	167.48	148.87
Salihli/Turgutlu area							
SR-1	82.03	173.93	0.47	0.54	100.60	129.34	114.97
SR-2	62.06	132.26	0.36	0.38	76.11	97.86	86.98
SR-3	73.43	155.86	0.42	0.49	90.05	115.78	102.92
SR-4	77.10	164.02	0.44	0.52	94.55	121.57	108.06
TR-1	66.16	136.18	0.37	0.42	81.14	104.33	92.74

kg and these values are lower than the recommended maximum value of 370 Bq/kg (OECD, 1979; Beretka and Mathew, 1985). To limit the annual external gamma-ray dose (UNSCEAR, 1982) to 1.5 mGy for the samples under investigation, the external hazard index (Hex) is given by the following equation:

$$Hex = (AU/370) + (ATh/259) + (AK/4810), \quad (6)$$

where *AU*, *ATh*, and *AK* are the activity concentrations of ^{226}Ra, ^{228}Ac, and ^{40}K, respectively. The results of Hex based on the Eq. (6) are given in Table 5. The results range from 0.15 to 0.83. Besides these, the gamma index (I_γ) proposed by the European Commission (1999) is defined in order to evaluate gamma-ray radiation originating from building materials. It is given in Eq. (7):

$$(I_\gamma) = (AU/300) + (ATh/200) + (AK/3000) \quad (7)$$

where *AU*, *ATh*, and *AK* are the activity concentrations (Bq/kg) of ^{226}Ra, ^{228}Ac, and ^{40}K, respectively. The values of 300, 200, and 3000 Bq/kg, the activity concentration indices for building materials, were calculated for a dose criterion limit of 1 mSv/year as given by the European

Commission Report (1999). Table 5 indicates that I_γ values of samples are less than unity in granitoid samples. Therefore, most of the granitoid samples are safe and can be used as construction material without posing any significant radiological threat to the population.

Activity concentration values obtained from granitoids in western Turkey, except for the Karaburun and Turgutlu granitoids, are higher than global average ^{226}Ra (35 Bq/kg) and ^{228}Ac (32 Bq/kg) values given by UNSCEAR (2008) (Figure 5).

5. Conclusions

Some granitoids of western Turkey having diverse geological, mineralogical, and geochemical characteristics have been evaluated in terms of their natural radioactivity levels. Geochemical and natural radioactivity data from granite to dioritic rocks allow us to identify two end members. One is the Buldan metagranitoids, characterized by high SiO_2, K_2O, Rb, Th, and Y contents. Another is the Karaburun granodiorites, defined by low SiO_2, K_2O, Rb, Ba, Th, U, and Zr contents. Furthermore, the lowest ^{226}Ra, ^{228}Ac, and ^{40}K values occur in the Karaburun granitoids while the Buldan granitoids have the highest values, confirming that the silica-rich acidic granitoids contain higher natural radioactivity levels than silica-poor basic granitoids. Natural radioactivity levels of granitoids were considered to be closely associated with the abundance of radioactive elements in some accessory minerals. However, the correlation of mineralogical, geochemical, and radiological data points out that the high natural radioactivity levels of these granitoids appear to be closely associated with high SiO_2, Na_2O, K_2O, Rb, and Ba contents, which may be a confirmation of a link to the late-phase enrichment of radioactive elements during or after emplacement of granitoid plutons.

Measured ^{226}Ra, ^{228}Ac, and ^{40}K radioactivity concentrations values are similar to the concentrations measured worldwide for ^{40}K, ^{226}Ra, and ^{232}Th, reported by UNSCEAR. The radiological parameters and radiation hazard index of granitoids indicate that these granitoids are

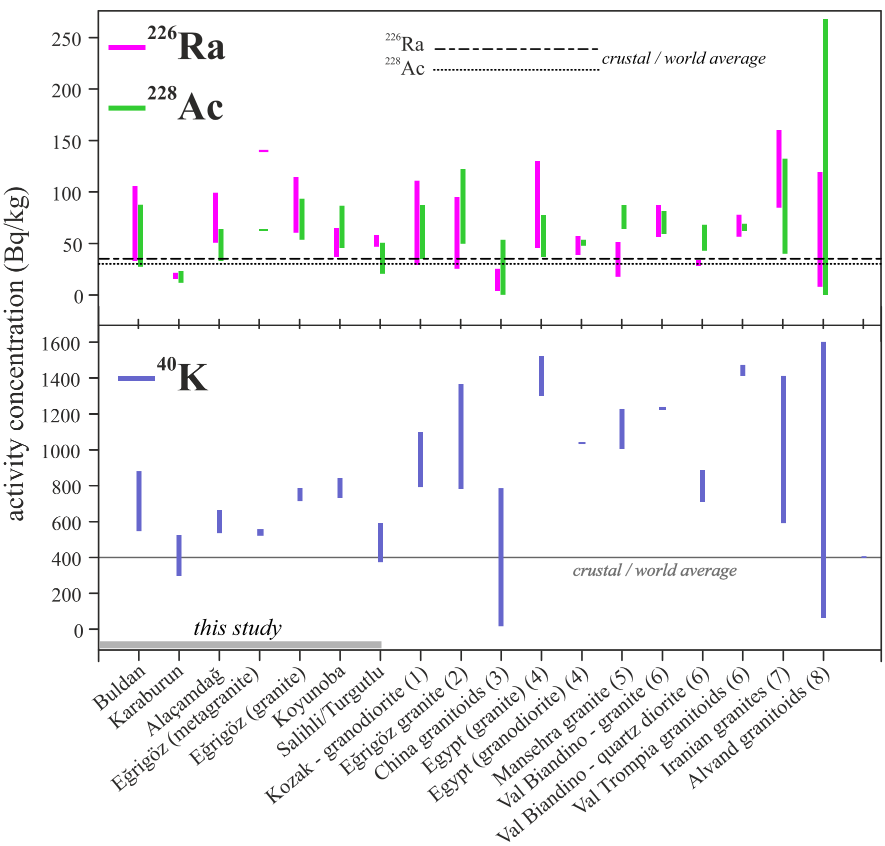

Figure 5. Correlation of activity concentration results between western Anatolian and Eurasian granitoids. Natural radioactivity values are from: (1) Karadeniz et al. (2011), (2) Öztürk et al. (2015), (3) Xinwei et al. (2006), (4) El-Arabi et al. (2007), (5) Qureshi et al. (2014), (6) De Capitani et al. (2007), (7) Jahangiri and Ashrafi (2011), (8) Pourimani et al. (2014).

safe for use as construction materials according to the dose criteria limits proposed by the OECD and the European Commission. Although radioactivity values are within safe limits, late-stage enrichment processes associated with metamorphism and hydrothermal alteration might have led to the enrichment of radioactive elements. Hence, granitoids that have undergone some alteration and incompatible element enrichment should be evaluated with caution in order to be used for industrial purposes.

Acknowledgments
The authors would like to thank the editor, Sabah Yılmaz Şahin, and the anonymous reviewers for their patience and valuable comments that greatly improved the manuscript. Whole-rock geochemical analyses of the granitoids were provided by research projects supported by the Scientific and Technological Research Council of Turkey (TÜBİTAK), Dokuz Eylül University, Akdeniz University, and Cumhuriyet University. Cihan Çolak and Selin Bilgiç are acknowledged for their assistance during sample preparation.

References

Ahmed NK (2005). Measurement of natural radioactivity in building materials in Qena city Upper Egypt. J Environ Radioact 83: 91-99.

Alharbi WR, Al Zahrani JH, Abbady AGE (2011). Assessment of radiation hazard indices from granite rocks of the Southeastern Arabian Shield, Kingdom of Saudi Arabia. Aust J Basic Appl Sci 5: 672-682.

Attendorn HG, Bowen R (1994). Isotopes in the Earth Sciences. Amsterdam, the Netherlands: Springer.

Beretka J, Mathew PJ (1985). Natural radioactivity of Australian building materials, industrial wastes and by-products. Health Phys 48: 87-95.

Blundy J, Wood B (2003). Partitioning of trace elements between crystals and melts. Earth Planet Sci Lett 210: 383-397.

Canbaz B, Çam F, Yaprak G, Candan O (2010). Natural radioactivity (^{226}Ra, ^{232}Th and ^{40}K) and assessment of radiological hazards in the Kestanbol granitoid, Turkey. Radiat Prot Dosim 141: 192-198.

Çetin E, Altınsoy N, Örgün Y (2012). Natural radioactivity levels of granites used in Turkey. Radiat Prot Dosim 151: 299-305.

Collins GL (1999). Equal time for the origin of granite - a miracle. Reports of the National Center for Science Education 19: 20-28.

De Capitani L, Carnevale M, Fumagalli M (2007). Gamma-ray spectroscopy determination of radioactive elements in late-Hercynian plutonic rocks of Val Biandino and Val Trompia (Lombardia, Italy). Period Mineral 76: 25-39.

Deer WA, Howie RA, Zussman J (2001). Rock-Forming Minerals, Volume 4A: Framework Silicates – Feldspars. 2nd ed. London, UK: Geological Society of London.

Delaloye M, Bingöl E (2000). Granitoids from Western and Northwestern Anatolia: Geochemistry and modeling of geodynamic evolution. Int Geol Rev 42: 241-268.

Doventon JH, Prensky SE (1992). Geological applications of wireline logs: A synopsis of developments and trends. Log Analyst 33: 286-303.

El-Arabi AM, Abbady AGE, Khalifa IH (2007). Radioactive and geochemistry characteristics of the garnetiferous granite of Um Sleimat area, Egypt. Online Journal of Earth Sciences 1: 9-20.

El Feky MG, El Mowafy AA, Abdel Warith A (2011). Mineralogy, geochemistry, radioactivity and environmental impacts of Gabal Marwa granites, southeastern Sinai, Egypt. Chinese J Geochem 30: 175-186.

Erkül F, Erkül ST, Ersoy Y, Uysal İ, Klötzli U (2013). Petrology, mineral chemistry and Sr-Nd-Pb isotopic compositions of granitoids in the Central Menderes Metamorphic Core Complex: constraints on the evolution of Aegean lithosphere slab. Lithos 180-181: 74-91.

Erkül ST (2012). Petrogenetic evolution of the Early Miocene Alaçamdağ volcano-plutonic complex, northwestern Turkey: implications for the geodynamic framework of the Aegean region. Int J Earth Sci 101: 197-219.

Erkül ST, Erkül F (2012). Magma interaction processes in syn-extensional granitoids: the Tertiary Menderes Metamorphic Core Complex, Western Turkey. Lithos 142-143: 16-33.

Erkül ST, Sözbilir H, Erkül F, Helvacı C, Ersoy Y, Sümer Ö (2008). Geochemistry of I-type granitoids in the Karaburun Peninsula, West Turkey: evidence for Triassic continental arc magmatism following closure of the Palaeotethys. Island Arc 17: 394-418.

European Commission (1999). Radiation Protection 112. Radiological Protection Principles Concerning the Natural Radioactivity of Building Materials. Brussels, Belgium: Directorate-General Environment, Nuclear Safety and Civil Protection.

Faure G (1986). Principles of Isotope Geology. New York, NY, USA: Wiley.

Gilmore GR (2008) Practical Gamma-Ray Spectroscopy. 2nd ed. Chichester, UK: John Wiley.

Jahangiri A, Ashrafi S (2011). Natural radioactivity in Iranian granites used as building materials. J Environ Stud 36: 16-18.

Karadeniz Ö, Akal C (2014). Radiological mapping in the granodiorite area of Bergama (Pergamon)-Kozak, Turkey. J Radioanal Nucl Ch 302: 361-373.

Karadeniz Ö, Çıyrak N, Yaprak G, Akal C (2011). Terrestrial gamma exposure in the granodiorite area of Bergama (Pergamon) – Kozak, Turkey. J Radioanal Nucl Ch 288: 919–926.

Kovler K (2012). Radioactive materials. In: Pacheco-Torgal F, Jalali S, Fucic A, editors. Toxicity of Building Materials. Cambridge, UK: Woodhead Publishing, pp. 196-240.

Krieger R (1981). Radioactivity of construction materials. Betonwerk Fertigteil Technology 47: 468-473.

Mason B, Moore CB (1982). Principles of Geochemistry. New York, NY, USA: Wiley & Sons.

Middlemost EAK (2013). Magmas, Rocks and Planetary Development: A Survey of Magma/Igneous Rock Systems. London, UK: Routledge Taylor and Francis Group.

MTA (1964). Geological Map of Turkey-İzmir, Denizli (1:500.000). Ankara, Turkey: Mineral Research and Exploration Institute of Turkey.

OECD (1979) Nuclear Energy Agency. Exposure to Radiation from Natural Radioactivity in Building Materials. Report by NEA Group of Experts. Paris, France: OECD.

Örgün Y, Altınsoy N, Gültekin AH, Karahan G, Çelebi N (2005). Natural radioactivity levels in granitic plutons and groundwaters in southeast part of Eskişehir, Turkey. Appl Radiat Isotopes 63: 267-275.

Örgün Y, Altınsoy N, Şahin SY, Güngör Y, Gültekin AH, Karahan G, Karacık Z (2007). Natural and anthropogenic radionuclides in rocks and beach sands from Ezine region (Çanakkale), Western Anatolia, Turkey. Appl Radiat Isotopes 65: 739-747.

Osmanlıoğlu AE (2006). Natural radioactivity and evaluation of effective dose equivalent of granites in Turkey. Radiat Prot Dosim 121: 325-329.

Özmen SF, Boztosun I, Yavuz M (2013). Determination of gamma radioactivity Levels and associated dose rates of soil samples of the Akkuyu/Mersin using high-resolution gamma-ray spectrometry. Rad Prot Dosim 158: 461-465.

Öztürk BC, Yaprak G, Çam NF, Candan O (2015). A radiological survey of the Eğrigöz granitoid, western Anatolia/Turkey. Rad Prot Dosim 164: 510-518.

Pagel M (1982). The mineralogy and geochemistry of uranium, thorium, and rare-earth elements in two radioactive granites of the Vosges, France. Mineral Mag 46: 149-161.

Papadopoulos A, Christofides G, Koroneos A, Papadopoulou L, Papastefanou C, Stoulos S (2013). Natural radioactivity and radiation index of the major plutonic bodies in Greece. J Environ Radioactiv 124: 227-238.

Pavlidou S, Koroneos A, Papastefanou C, Christofides G, Stoulos S, Vavelides M (2006). Natural radioactivity of granites used as building materials. J Environ Radiactiv 89: 48-60.

Pourimani R, Ghahri R, Zarel MR (2014). Natural radioactivity concentrations in Alvand granitic rocks in Hamadan, Iran. Rad Prot Environ 37: 132-142.

Qureshi AA, Tariq SA, Ud Din K, Manzoor S, Calligaris C, Waheed A (2014). Evaluation of excessive lifetime cancer risk due to natural radioactivity in the rivers sediments of Northern Pakistan. J Rad Res Appl Sci 7: 438-447.

Rankama K, Sahama TG (1950). Geochemistry. Chicago, IL, USA: University of Chicago Press and Cambridge University Press.

Rizzo S, Brai M, Basile S, Bellia S, Hauser S (2001). Gamma activity and geochemical features of building materials: estimation of gamma dose rate and indoor radon levels in Sicily. Appl Radiat Isot 55: 259-265.

Rogers JJW, Ragland PC (1961). Variation of thorium and uranium in selected granitic rocks. Geochim Cosmochim Ac 25: 99-109.

Rudnick RL, Gao S (2003). Composition of the continental crust. In: Rudnick RL, editor. The Crust. Amsterdam, the Netherlands: Elsevier, pp. 1-64.

Sayın N (2013). Radioactive element contents of some granites used as building materials: insights into the radiological hazards. Bull Eng Geol Environ 72: 579-587.

Streckeisen A (1976). To each plutonic rock its proper name. Earth-Sci Rev 12: 1-33.

Taylor SR, McLennan SM (1985). The Continental Crust: Its Composition and Evolution. Oxford, UK: Blackwell Scientific Publications.

Turcotte D, Schubert G (2002). Geodynamics. 2nd ed. Cambridge, UK: Cambridge University Press.

Tzortzis M, Haralabos T, Christofides S, Christodoulides G (2003). Gamma radiation measurements and dose rates in commercially used natural tiling rocks (granites). J Environ Radioact 70: 223-235.

UNSCEAR (1982). Ionizing Radiation: Sources and Biological Effects. Annex B, D. New York, NY, USA: United Nations.

UNSCEAR (1988), Report to the General Assembly. New York, NY, USA: United Nations.

UNSCEAR (1993). Exposure from Natural Sources of Radiation. Report to the General Assembly, with Scientific Annexes. New York, NY, USA: United Nations.

UNSCEAR (2000). Sources and Effects of Ionizing Radiation. Report to the General Assembly, with Scientific Annexes. United Nations Sales Publication E.00.IX.3. New York, NY, USA: United Nations.

UNSCEAR (2008). Sources of Ionizing Radiation, Report Vol. I, II. Annex, B, D. New York, NY, USA: United Nations.

Xinwei LW, Lingqing J, Xiaodan Y, Leipeng S, Gelian D (2006). Specific activity and hazards of Archeozoic-Cambrian rock samples collected from the Weibei area of Shaanxi, China. Radiat Prot Dosim 118: 352-359.